BRCT Domain Interactions in the Heterodimeric DNA Repair Protein XRCC1−DNA Ligase III[†]

Anna Dulic,[‡] Paul A. Bates,[§] Xiaodong Zhang,[∥] Stephen R. Martin,[⊥] Paul S. Freemont,[∥] Tomas Lindahl,*[,‡] and Deborah E. Barnes[‡]

Mutagenesis Laboratory, Imperial Cancer Research Fund, Clare Hall Laboratories, Blanche Lane, South Mimms, Hertfordshire, EN6 3LD, U.K., Biomolecular Modeling, and Molecular Structure and Function Laboratories, Imperial Cancer Research Fund, 44 Lincoln's Inn Fields, London, WC2A 3PX, and Division of Physical Biochemistry, National Institute for Medical Research, The Ridgeway, Mill Hill, London NW7 1AA.

Received November 27, 2000; Revised Manuscript Received March 13, 2001

ABSTRACT: Proteins involved in DNA repair, or its coordination with DNA replication and mitosis through cell cycle checkpoints, are vital in the concerted cellular response to DNA damage that maintains the integrity of the genome. The "BRCT" domain (BRCA1 carboxy terminal) was noted as a putative protein−protein interaction motif in the breast cancer suppressor gene, *BRCA1*, and subsequently identified in over 50 proteins involved in DNA repair, recombination, or cell cycle control. The heterodimer of the DNA repair proteins, XRCC1 and DNA ligase III, was the first example of a functional interaction via BRCT modules. The only three-dimensional crystal structure of a BRCT domain was solved for this region of XRCC1. Key amino acid residues mediating the interaction with DNA ligase III were identified here by targeted mutagenesis of the XRCC1 BRCT domain. The consequences of these mutations on protein folding were assessed. A structural model of the DNA ligase III BRCT domain was constructed and similarly tested by mutation of corresponding residues required for the interaction with XRCC1. These data identify the XRCC1-DNA ligase III heterodimer interface and provide the first demonstration of the surface contacts coordinating a functional BRCT−BRCT protein interaction.

The BRCT motif was first identified in the C-terminus of the product of the *BRCA1* breast cancer suppressor gene (BRCA1 carboxy terminal), as a putative autonomously folding domain of ∼95 amino acids containing distinctive hydrophobic clusters (*1*). Database searches have identified to date over 50 proteins with BRCT domains, involved in either DNA repair, recombination, and/or cell cycle control. BRCT domains were predicted to function in protein−protein interactions but no direct biochemical evidence was initially available (*1*−*3*). The DNA base excision-repair (BER)[1] pathway is coordinated at a base lesion by sequential pairwise interactions of the component repair proteins (*4*). Of these, only XRCC1 and DNA ligase III normally exist as a preformed complex in vivo (*5*). They strongly interact with each other via their respective C-terminal sequences forming a heterodimer (*6*); these regions correspond to BRCT domains. This provided evidence that BRCT domains represent important adaptor units in eukaryotic DNA repair proteins and can mediate protein−protein interactions between components of the repair machinery (*7*).

XRCC1 was originally identified by its ability to correct a mutant cell line, EM9, hypersensitive to alkylating agents and ionizing radiation and unable to rejoin single-strand breaks resulting from such damage (*8*, *9*). No enzymatic activity has been assigned to XRCC1, and it appears to act as a scaffold protein during BER (*4*). XRCC1 was shown to be required for maintaining stability and normal levels of DNA ligase III in vivo (*5*). There are two alternatively spliced forms of DNA ligase III detected in mammalian tissues, a 102 kDa (α) form that is present in all tissues and functions in short-patch BER and a 96 kDa (*β*) form that occurs only in testis and may play a role in meiotic recombination (*10*, *11*). These two isoforms differ at their C-termini, and the shorter form of DNA ligase III does not bind to XRCC1 (*6*). A distinct, centrally located BRCT domain in XRCC1 interacts with poly(ADP-ribose) polymerase (*12*), while XRCC1 also binds to both DNA polymerase *β* and nicked/gapped DNA via different contacts in its non-BRCT N-terminal domain (*13*). XRCC1 has been shown to have an additional S phase-specific role in DNA strand-break repair, independently of DNA ligase III (*14*) and to be essential for early embryonic development in mice (*15*).

Informative insights into the function of the BRCT motif have come from the first three-dimensional (3D) crystal structure, which was solved for a homodimer of the C-terminal BRCT domain of XRCC1 (*16*). The structure predicted a compact globular domain for each monomer comprised of a core four-stranded parallel *β*-sheet surrounded by three α-helices (Figure 1). Helices α1 and α3 contain

[†]This work was supported by the Imperial Cancer Research Fund.

* To whom all correspondence should be addressed. Phone: +44-20-7269-3993. Fax: +44-20-7269-3819. E-mail: lindahl@icrf.icnet.uk.

[‡] Mutagenesis Laboratory.

[§] Biomolecular Modeling Laboratory.

[∥] Molecular Structure and Function Laboratory.

[⊥] Division of Physical Biochemistry.

[1] Abbreviations: BER, base excision repair; 3D, three-dimensional; PCR, polymerase chain reaction; IPTG, isopropyl *β*-D-thiogalactoside; NTA, nitrilotriacetic acid; BSA, bovine serum albumin; SDS−PAGE, sodium dodecyl sulfate−polyacrylamide gel electrophoresis; BCIP, 5-bromo-4-chloro-3-indolyl phosphate; NBT, nitro blue tetrazolium; UV, ultraviolet; CD, circular dichroism.

10.1021/bi002701e CCC: $20.00
Published on Web 04/28/2001

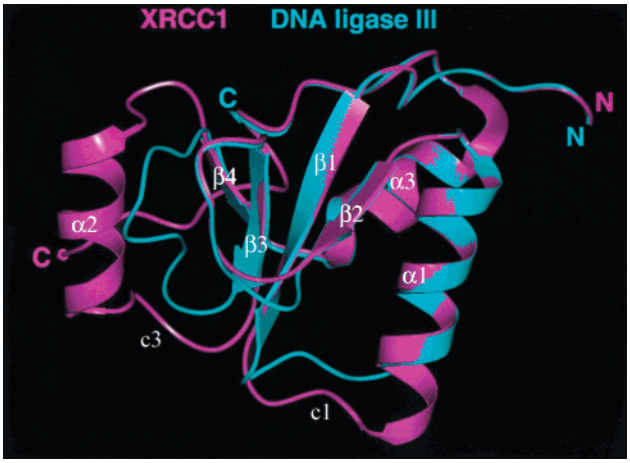

FIGURE 1: Model of the DNA ligase III BRCT domain. Ribbon representation of the modeled DNA ligase III BRCT domain (cyan), superimposed on the XRCC1 BRCT structure (consisting of a four-stranded parallel β-sheet, surrounded by three α-helices, as shown in magenta; surface loops c1 and c3 are indicated). N- and C-termini are labeled.

residues conserved among the BRCT family members that are predicted to be essential for the fold, and α1 also contributes key residues to the proposed XRCC1 homodimer interaction surface (*16*, *17*). Perhaps because of the hydrophobic nature and consequent poor solubility of isolated BRCT domains, attempts to crystallize this domain from other proteins (including BRCA1 itself) have been unsuccessful, so the XRCC1 BRCT structure provides the prototype for modeling other BRCT domains. Thus, it was possible to predict the structure of the C-terminal BRCT domain of BRCA1 and interpret various mutations that have been reported to predispose to breast cancer (*16*). In view of the limited primary amino acid sequence conservation between BRCT proteins, the 3D structure now allows an informed approach to targeted mutagenesis experiments with the various family members.

Here, site-specific mutagenesis has been used to test the predicted XRCC1 BRCT domain structure and fold and analyze the surface interaction between the BRCT domains of XRCC1 and DNA ligase III. The XRCC1 BRCT domain structure has also been used to model the DNA ligase III BRCT domain and putative heterodimer interface, which were similarly tested.

EXPERIMENTAL PROCEDURES

XRCC1 and DNA ligase III Mutations. Minimal XRCC1 and DNA ligase III constructs containing the respective BRCT domains were as previously described (*6*). Briefly, the XRCC1 construct was comprised of the C-terminal 96 amino acids of the full-length protein (residues 538−633) fused to a C-terminal FLAG marker octapeptide (N-AspTyrLysAspAspAspAspLys-C; Eastman Kodak Co.). The DNA ligase III construct was comprised of the C-terminal 149 amino acids of DNA ligase IIIα (residues 774−922) fused to an N-terminal 10× histidine tag. Residues in these two interacting BRCT domains were numbered 1−96 and 1−149, excluding the tags, to conform with the numbering system used previously for the 3D structure of the XRCC1 BRCT domain (16). All mutations were introduced using the QuickChange Site-Directed Mutagenesis Kit, according to the manufacturer's instructions (Stratagene). Up to four base changes were introduced with one mutagenic primer. Sense primers are shown in coding triplets with mutated bases underlined: (a) for XRCC1 mutants, Thr30Ala31 to ArgArg, 5′-CTC ATC CGA TAC GTC CGA CGC TTC AAT GGG GAG CTC GAG-3′; Leu2 to His, 5′-CC ATG GCT GAG CAC CCA GAT TTC TTC CAG G-3′; Arg23Arg27 to GluGlu, 5′-GGG GAC GAG CGG GAG AAA CTC ATC GAA TAC GTC ACA GCC-3′; Trp74 to Leu, 5′-GCA TTC GTT CGT CCC CGA TTG ATC TAC AGT TGC-3′; Trp74 to Asp, 5′-CC CTG GCA TTC GTT CGT CCC CGA GAT ATC TAC AGT TGC-3′; Ile48 to Glu, 5′-C CGG GTT CAG TTT GTG GAG ACA GCA CAG GAA TGG G-3′; Leu85 to His, 5′-G AAG CAG AAG TTA CAT CCT CAC CAG CTC TAT GGG-3′; Asp20 to Ala, 5′-G TTC CCT GGG GCC GAG CGG CGG AAA CT C-3′; Glu59 to Lys, 5′-G GAT CCC AGC TTT GAG AAG GCC CTG ATG GAC-3′; (b) for DNA ligase III mutants, Trp63 to Leu, 5′-CAG GTC TCC CCA GAG TTG ATT TGG GCA TG-3′; Leu2 to His, 5′-CG CTG TGC CAA ACA AAG GTA CAC CTG GAC ATC TTC ACT GGG-3′; Asp19 to Ala, 5′-CCC TCC ACA CCA GCC TTC AGC CGT CTC-3′. All constructs were sequenced to check for the presence of the desired mutation(s) and the absence of any additional changes due to PCR errors.

Purification of Recombinant BRCT Domains. All constructs were transformed into the *Escherichia coli* strain BL21(DE3) and recombinant BRCT domains overexpressed by IPTG induction. BRCT domains were affinity purified using either anti-FLAG M2 affinity gel (Eastman Kodak Co.) in the case of XRCC1 mutants or Ni-NTA-agarose (Qiagen) in the case of DNA ligase III mutants, as previously described (*6*). Centricon microconcentrators (Amicon Inc.) were preblocked in 1% dried milk and used to concentrate and buffer exchange (in the case of DNA ligase III constructs) BRCT domains produced. In the case of XRCC1 constructs, the FLAG peptide used for the elution of these BRCT domains was also removed at this stage. Amino acid changes were confirmed by mass spectrometric analysis of tryptic digests of the recombinant BRCT domains, as described by van Ham et al. (*18*).

Co-Affinity Precipitation Assay. Binding of His-DNA ligase III and XRCC1−FLAG BRCT domains was detected as described previously (*6*). Briefly, the DNA ligase III BRCT domain (2 μg) was incubated with the XRCC1 BRCT domain (2 μg) and BSA (1 μg) in a reaction (11 μL volume) containing 50 mM Tris-HCl, pH 7.5, 100 mM NaCl, 10% glycerol, 1 mM EDTA, 1 mM DTT at 20 °C for 20 min. Ni-NTA-agarose beads (25 μL bed volume) at pH 8 were added to the reaction and incubated for a further 20 min. Beads were washed six times with 105 μL of 25 mM imidazole followed by two 35 μL elutions of 250 mM imidazole. Thirty μL of each of the six washes and two elutions were fractionated by SDS−PAGE. Recovery of the His-DNA ligase III BRCT domain on Ni-NTA-agarose beads was monitored by silver staining or immunoblotting with anti-peptide antibodies against amino acids 882−897 of DNA ligase IIIα (*6*); the XRCC1 BRCT domain was detected by immunoblotting with the anti-FLAG M2 monoclonal antibody (Eastman Kodak Co.). Alkaline phosphatase-conjugated secondary antibodies (Bio-Rad) and BCIP/NBT substrate (Sigma) were employed in all cases.

Comparative Modeling of the BRCT Domain of DNA ligase III. The model of the DNA ligase III BRCT domain was constructed using the C-terminal XRCC1 BRCT domain crystal structure as a template (*16*). The amino acid sequence alignment of the DNA ligase III and XRCC1 BRCT domains was derived manually, taking into consideration the alignment of all BRCT family members in the Pfam database (www.sanger.ac.uk/cgi-bin/pfam) and features of the XRCC1 BRCT domain crystal structure, e.g., conserved and buried hydrophobic residues. The program, 3D-JIGSAW, was used to replace loops and regions with incompatible backbone angles to the template, and for refinement of side-chain rotamers (*19*). To remove the small number of steric clashes remaining in the model, 100 steps of steepest descents were run using the program CHARMM (ver. 3.3; Molecular Simulations Inc., 200 Fifth Avenue, Waltham, MA). The Protein health checks option in the program QUANTA (ver. 3.3; Molecular Simulations Inc.) was used to check the general packing quality of the protein core; the model passed all filters, such as excess volume within the core and close contacts. The program PROCHECK (*20*) was also used to check stereochemical quality of the model (see ref *21*, for a detailed assessment of comparative modeling).

Circular Dichroism and Thermal Denaturation. BRCT domain protein concentrations were estimated from absorption spectra using calculated extinction coefficients (*22*). Far-UV circular dichroism (CD) measurements were performed using a Jasco J-715 spectropolarimeter. The spectra were recorded at 20 °C using 1 mm fused silica cuvettes with XRCC1 BRCT domain concentrations in the range 7−12 μM. For each spectrum, four scans were averaged and the baseline subtracted. CD intensities are presented as the CD absorption coefficient calculated using the molar concentration of protein ($\Delta\epsilon_M$) rather than on a mean residue weight (MRW) basis. Values of $\Delta\epsilon_{MRW}$ may be calculated as $\Delta\epsilon_{MRW} = \Delta\epsilon_M/N$ (where N should be the appropriate number of peptide bonds). For thermal unfolding experiments, the CD intensity was monitored at 223 nm on heating XRCC1 BRCT domain solutions from 10 to 90 °C at ~1 °C min^{-1}. The sample temperature was measured using an immersed thermocouple (Comark).

RESULTS

Amino Acid Substitutions in the BRCT Domain of XRCC1 Affecting the Proposed Dimer Interface and Its Interaction with DNA Ligase III. The minimal fragment of XRCC1 that is sufficient for interaction with DNA ligase III was defined as the C-terminal 96 amino acids of the protein (*6*). The BRCT crystal structure was solved for a homodimer of the XRCC1 domain, formed through interactions between both α1 and the N-terminal region of each monomer (*16*). Sequence similarities between the BRCT domains of XRCC1 and DNA ligase III indicated that some of the interactions in the XRCC1 dimer interface could be retained in the biologically relevant heterodimeric BRCT complex between XRCC1 and DNA ligase III. This has been tested directly here by mutating key residues at the XRCC1 dimer interface (Table 1 and Figure 2A). The ability of these purified mutant BRCT domains to interact with the minimal domain of DNA ligase III (C-terminal 149 amino acids) was tested by a co-affinity precipitation assay (*6*). C-Terminal FLAG-tagged wild-type and mutant XRCC1 BRCT domains were incubated with the N-terminal His-tagged DNA ligase III BRCT domain, then the DNA ligase III and any interacting XRCC1 were recovered on nickel agarose beads. Recovery of the DNA ligase III BRCT domain was confirmed by silver staining (Figure 3A) and co-affinity precipitation of the XRCC1 BRCT domain detected by immunoblotting with an anti-FLAG antibody (Figure 3B), after separation of samples by SDS−PAGE.

Table 1: Mutations Introduced in the BRCT Domain of XRCC1 and Their Effects on the Interaction with DNA Ligase III

XRCC1 mutations[a]	proposed role of the mutated residue(s)	location in XRCC1 BRCT domain	interaction with DNA ligase III BRCT domain
wild-type	N/A	N/A	+
Thr30Ala31 to ArgArg	hydrophobic, dimer interface	α1	−
Leu2 to His	(as above)	N-terminus	−
Arg23Arg27 to GluGlu	salt-bridge, dimer interface	α1	−
Trp74 to Leu	most conserved, hydrophobic core	α3	−
Trp74 to Asp	(as above)	α3	−
Ile48 to Glu	hydrophobic core	β3	−
Leu85 to His	positioning C-terminus onto core	C-terminus	+
Asp20 to Ala	equivalent to BRCA1 mutation	α1	+
Glu59 to Lys	(control)	α2	+

[a] Amino acid residues are numbered within the BRCT domain (*16*); N/A = not applicable.

Thr30, Ala31, and Leu2 in the XRCC1 BRCT domain were mutated to basic residues (Table 1 and Figure 2A) to disrupt hydrophobic dimer surface interactions revealed in the 3D structure (*16*). The heterodimer appears to be coordinated by such hydrophobic interactions, forming more efficiently at 20 °C than at 0 °C in vitro and is resistant to 2 M salt (*23*). However, the heterodimer interaction is not perturbed by nonionic detergent (Nonidet P40 ≤ 2% v/v; data not shown). Substitution of Thr30 and Ala31 abrogated the interaction with the DNA ligase III BRCT domain, as indicated by inability to recover the mutant XRCC1 BRCT domain (Figure 3, panels C and D). Similar results were obtained for the Leu2 mutant. Mutations altering the charge of Arg23 and Arg27 by replacements with Glu (Table 1 and Figure 2A) also abolished interaction between the BRCT domains of XRCC1 and DNA ligase III; in the XRCC1 BRCT domain homodimer, these residues were thought to coordinate salt bridges across the α1-α1 dimer interface through hydrogen bonds (Arg23···Glu35; Arg27···Asp4, Asn33) with the other monomer (*16*, *17*).

The absence of detectable mutants in elutions here indicates that the amount bound to DNA ligase III was greatly reduced compared to the wild-type XRCC1 BRCT domain (compare Figure 3, panels B and D, elutions). However, estimation of a dissociation constant for the XRCC1−DNA ligase III interaction is not possible, as it is unclear whether all molecules are accessible for heterodimer formation. This may be particularly true for XRCC1 as, even for the wild-type BRCT domain, only ~10% binds the DNA ligase III BRCT domain in the in vitro co-affinity precipitation assay (*6*; compare Figure 3B, washes 1 and 2 vs elutions). This is most likely due to formation of an XRCC1 BRCT homodimer (*16*), which compromised attempts to quantify the XRCC1−DNA ligase III BRCT−BRCT inter-

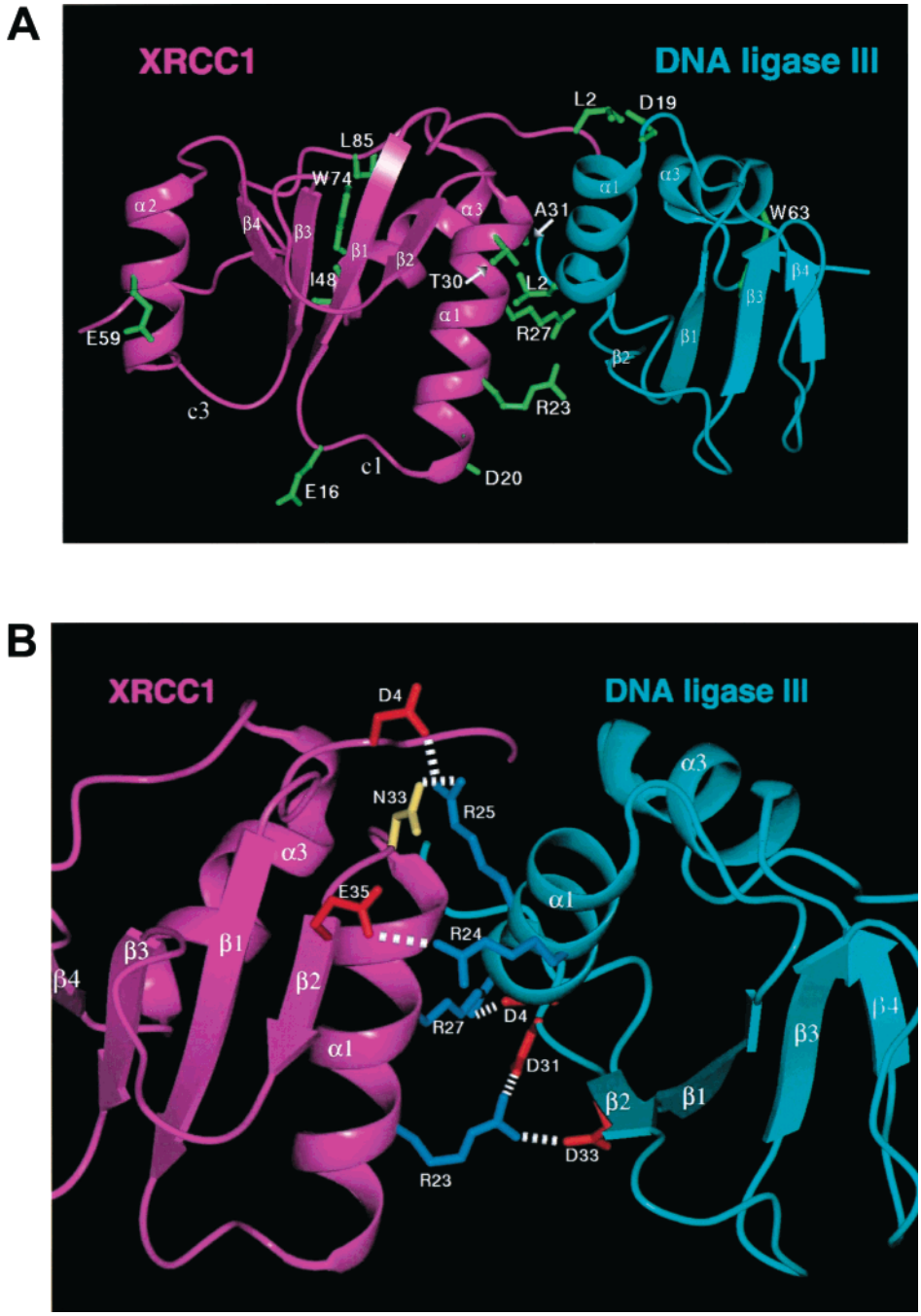

FIGURE 2: Structural model of the XRCC1-DNA ligase III BRCT domain heterodimer. (A) Proposed model of the XRCC1-DNA ligase III interaction. Key residues indicated here in green were targeted in site-directed mutagenesis experiments. (B) Salt-bridge interactions between the two different monomers at the α1-α1 heterodimer interface. Amino acid side-chains are colored: acidic (red), basic (blue), polar (yellow). Residues are numbered within the BRCT domains (*16*). Single letter amino acid code is used here due to restricted space.

action by surface plasmon resonance measurements using the Biacore 3000 system (Biacore AB).

Effects of Site-Specific Mutations of Core Residues in the BRCT Domain of XRCC1. Trp74 in the XRCC1 BRCT domain is the most invariant residue among the BRCT family members (*2*, *3*) and is located in α3 at the center of a highly conserved hydrophobic pocket, interacting with other conserved residues in the *β*-sheets, as well as the C-terminal tail (*16*; Figures 1 and 2A). Substitution of this residue with either Leu (maintaining hydrophobicity) or an acidic residue, Asp, yielded mutant domains that were unable to bind to DNA ligase III, giving analogous results to those obtained for the XRCC1 dimer interface mutants (see Figure 3, panels C and D). Similarly, the interaction was abolished when Ile48 in the XRCC1 BRCT domain was mutated to Glu (Table 1, Figure 2A). Ile48 is also located in the hydrophobic core of the domain and was shown previously to affect the interaction with DNA ligase III when mutated to an acidic residue (*24*). Surprisingly, in the same study, Taylor et al. (*24*) reported that substitution of Trp74 with Asp did not affect the interaction of XRCC1 with DNA ligase III, in conflict with the present results, although expression of the Trp74 to Asp XRCC1 protein failed to restore repair in noncycling *xrcc1* mutant cells (25).

Additional Informative Amino Acid Substitutions in the XRCC1 BRCT Domain. Further amino acid substitutions

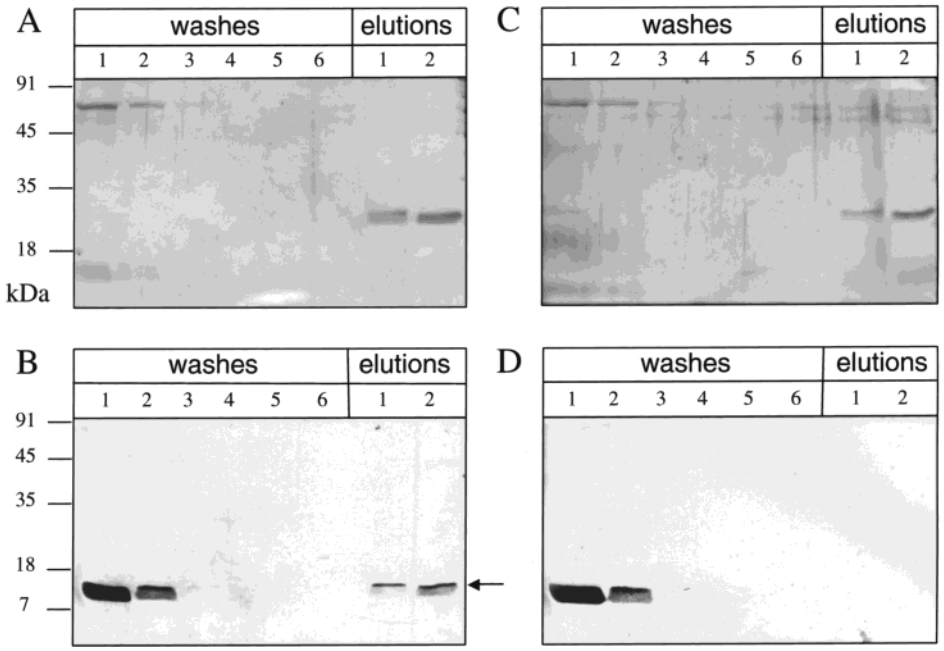

FIGURE 3: Analysis of the effects of mutations in the BRCT domain of XRCC1 on the interaction with DNA ligase III. Typical results are shown for the binding, or absence of detectable binding, between the BRCT domain of XRCC1 (A and B), or an XRCC1 mutant (Thr30Ala31 to ArgArg; C and D), and the DNA ligase III BRCT domain in the co-affinity precipitation assay. The tagged BRCT domains, XRCC1−FLAG and His-DNA ligase III, were incubated in the presence of BSA and further incubated with Ni-NTA-agarose beads. Beads were washed six times with 25 mM imidazole to remove nonspecifically associated protein, and bound DNA ligase III was eluted (2×) in 250 mM imidazole (as indicated). Protein domains were fractionated by SDS−PAGE. Recovery of the bound His-DNA ligase III in elutions was monitored by silver staining (A and C); co-affinity precipitation of XRCC1-FLAG (arrowed) was monitored by Western blot with the anti-FLAG M2 antibody (B and D). BSA (69 kDa) was removed from the beads in the washes (A and C).

were made in the XRCC1 BRCT domain (Table 1, Figure 2A) to test various other features of the 3D structure. Mutation of Leu85 did not disrupt binding to DNA ligase III; this surface residue was proposed to be involved in positioning the C-terminal tail of the XRCC1 BRCT domain onto the hydrophobic core (*16*) but is not important for the heterodimer interaction. Interestingly, substitution of Asp20 in the XRCC1 BRCT domain, equivalent to Met1775 in BRCA1 that is commonly mutated in breast cancer (*16*), does not grossly affect interaction with DNA ligase III. BRCA1 interacts with different proteins to XRCC1 and the Met1775 residue is apparently involved in specific binding to these partners (*26*, *27*). The integrity of the two BRCT domains in BRCA1 is also crucial for transcription activation, and random mutagenesis with screening for loss of function preferably targeted hydrophobic residues in this region of the protein (*28*). Finally, substitution of Glu59 in the XRCC1 BRCT domain with Lys was included as a control (Table 1). This residue is located in α2, on the opposite face of the XRCC1 BRCT domain to the dimer interface (Figure 2A), thus would not be predicted to affect the interaction between XRCC1 and DNA ligase III, and results here confirmed this notion.

DNA Ligase III BRCT Domain Model and Effects of Site-Specific Mutations of Key Residues on Binding to XRCC1. A minimal functional domain of DNA ligase III, sufficient for interaction with the XRCC1 BRCT domain in vitro, was defined as the C-terminal 149 amino acids (*6*) and has been used in all functional studies. This is larger than the actual BRCT domain but shorter forms of the protein (or N-terminally extended versions) could not be overproduced, in various expression systems, in soluble quantities suitable for structural studies (data not shown). Instead, a 3D model for the BRCT domain of DNA ligase III was constructed based on the XRCC1 structure (*16*) and the shared 28% amino acid sequence identity of these two BRCT domains (see Experimental Procedures). Figure 1 shows the DNA ligase III model, superimposed on the XRCC1 BRCT domain structure. The four-stranded β-sheet and α1 and α3 helices are readily distinguished in the DNA ligase III domain, but not the α2 helix. Sequences corresponding to the α2 region are the least conserved within the BRCT family and are absent in some members, including DNA ligase III. The XRCC1 BRCT domain also has an extended C-terminal tail relative to that of DNA ligase III (Figure 1).

Two of the most conserved regions of structure in the BRCT domains of XRCC1 and DNA ligase III are the N-termini and the α1 helices; these are also the most conserved in primary sequence containing 60% of the amino acid identities. As the solved crystal structure of the XRCC1 BRCT domain showed interaction of a homodimer through these regions, this strongly suggested that the XRCC1−DNA ligase III heterodimer interface was similar. To test this, the model of the DNA ligase III BRCT domain was superimposed on one member of the XRCC1 homodimer (as in Figure 1) and the interface between the model and the second XRCC1 domain inspected (Figure 2A). This interface looked feasible, and it was clear that key salt-bridge interactions observed between XRCC1 monomers in the homodimer interface (Arg23···Glu35; Arg27···Asp4, Asn33; refs *16*, *17*) were maintained in the XRCC1-DNA ligase III heterodimer. Indeed, only a few side-chain angles needed to be readjusted to make good hydrogen-bonding contacts across the heterodimer interface, particularly between Arg23 of XRCC1···Asp31, Asp33 of DNA ligase III and Arg27···Asp4, but also between Asp4, Asn33 of XRCC1···Arg25 of DNA

Table 2: Mutations Introduced in the BRCT Domain of DNA Ligase III and Their Effects on the Interaction with XRCC1

DNA ligase III mutations[a]	interaction with XRCC1 BRCT domain	XRCC1 mutations (equivalent)
wild-type	+	wild-type
Trp63 to Leu	−	Trp74 to Leu
Leu2 to His	−	Leu2 to His
Asp19 to Ala	+	Asp20 to Ala

[a] Amino acid residues are numbered within the BRCT domain (*16*).

ligase III, and Glu35···Arg24 (Figure 2B). Disruption of the first two salt-bridges, by substitution of Arg23 and Arg27 in XRCC1 with acidic residues, abrogated heterodimer formation (see above). The buried surface at the BRCT domain heterodimer interface was 1460 Å^2, similar to the subunit interface of the XRCC1 homodimer, 1501 Å^2 (*17*), both of which are significant for a protein−protein interaction (*29*).

Mutations were introduced to test other key residues in the DNA ligase III BRCT domain (Table 2 and Figure 2A), including the core residue Trp63 (Trp74 in XRCC1), and hydrophobic Leu2 residue at the proposed interaction surface (Leu2 in XRCC1). Both these mutations abolished binding to XRCC1 in the co-affinity precipitation assay (Figure 4, panels C and D); interaction of the XRCC1-DNA ligase III BRCT domains was in this case monitored by immunoblotting of both proteins (Figure 4, panels A and B). Mutation of Asp19 in DNA ligase III, similarly to Asp20 in XRCC1, did not affect the heterodimer interaction (see above).

Protein Secondary Structure and Thermal Stability of Mutant XRCC1 BRCT Domains. The most invariant residue in the BRCT domain family (Trp74 in XRCC1, Trp63 in DNA ligase III) is not located on the surface but is buried inside the highly conserved hydrophobic core, and is predicted to hold the domain structure together (*16*). Trp74 in the XRCC1 BRCT domain is critical for the interaction with DNA ligase III (Table 1), substitutions of this residue presumably affecting the heterodimer interaction indirectly through changes in secondary structure. The CD spectra of proteins in the far-UV region of the spectrum (190−250 nm) derive principally from the amide chromophore and reflect protein α-helical structure. CD measurements have therefore been employed to investigate whether mutations (particularly substitution of Trp74) would affect this aspect of the secondary structure of the XRCC1 BRCT domain. All the mutants studied gave far-UV CD spectra with similar band shape and intensity (Figure 5); the slightly different band shape observed for the two Trp mutants is consistent with there being a small contribution from a Trp residue to the far-UV CD intensity (*30*). The magnitude of the signal for the wild-type XRCC1 BRCT domain indicates that some 25−30 residues are in a helical conformation, consistent with the known structure (*16*). The slight variations in intensity for the different mutants might indicate small differences in conformation but are probably accounted for by errors of ≤10% in the determination of protein concentrations. Thus, any change in helical content must be small (probably of the order of one helical turn) and none of the mutations have a major effect on the secondary structure of the XRCC1 BRCT domain. As some mutations, e.g., the Trp substitutions, were predicted to prevent proper folding of the domain, further measurements were made with the wild-type XRCC1 BRCT domain and the two Trp mutants to assess any effect of the Trp substitutions on thermal lability (Figure 6). The wild-type BRCT domain showed a cooperative unfolding transition in which the regular secondary structure was lost, typical of the conversion of a compactly folded, native protein to an unfolded, denatured state; the transition midpoint was at approximately 55 °C. The domain refolded upon lowering the temperature (data not shown). For the two Trp mutants, only small changes in the CD intensity were observed at temperatures greater than 50 °C; however, these changes were not reversed on lowering the temperature and the loss of signal at high temperatures is therefore probably due to protein aggregation.

DISCUSSION

The X-ray crystal structure of a BRCT domain had been determined but not previously tested by site-specific mutagenesis. Furthermore, the structure was solved for an XRCC1 BRCT domain homodimer, but identified conserved elements that might also mediate the BRCT heterodimer interaction of XRCC1 and its in vivo protein partner, DNA ligase III (*16*). The XRCC1 BRCT structure comprised a four-stranded parallel β-sheet surrounded by three α-helices (Figure 1), helices α1 and α3 containing conserved residues proposed to contribute to the BRCT protein fold. The α1 helix and N-terminus were predicted to form the XRCC1 BRCT homodimer interaction surface; these regions are the most highly conserved, in terms of amino acid sequence, between XRCC1 and DNA ligase III. Here, residues inferred from the XRCC1 BRCT domain structure to mediate surface interactions at the homodimer interface have been targeted by site-specific mutagenesis and shown to be necessary for the XRCC1−DNA ligase III heterodimer interaction. On the basis of the XRCC1 BRCT domain crystal structure and amino acid sequence homologies, a 3D model of the DNA ligase III BRCT domain has been constructed and similarly validated by site-specific mutagenesis. Thus, key residues revealed in the XRCC1 BRCT domain homodimer structure are conserved in the XRCC1−DNA ligase III model and had analogous effects on heterodimer formation when mutated in either protein. As in the XRCC1 homodimer, the XRCC1−DNA ligase III interaction is apparently coordinated by salt-bridges and key hydrophobic interactions across an essentially electrostatic α1−α1 BRCT interface (Figure 2).

The most highly conserved (Trp) residue in the BRCT protein family is not located at the interface but is buried in the hydrophobic core of the BRCT domain. In the 3D structure of the XRCC1 domain, the conserved hydrophobic clusters that constitute the BRCT sequence motif form the core β-sheet, C-terminal region, and α3 helix that are critical to the overall BRCT fold. Trp74 (in α3) was proposed to be a key residue essential to the correct folding of this hydrophobic core (*16*, *17*). Substitutions of this residue here abolished the XRCC1−DNA ligase III BRCT domain heterodimer interaction, presumably through changes in secondary structure; this was tested directly by biophysical techniques. Intriguingly, CD measurements did not detect any changes in α-helical structure in the XRCC1 Trp mutants. Although there was apparently no major disruption of the three α-helices, one of which (α1) forms the dimer

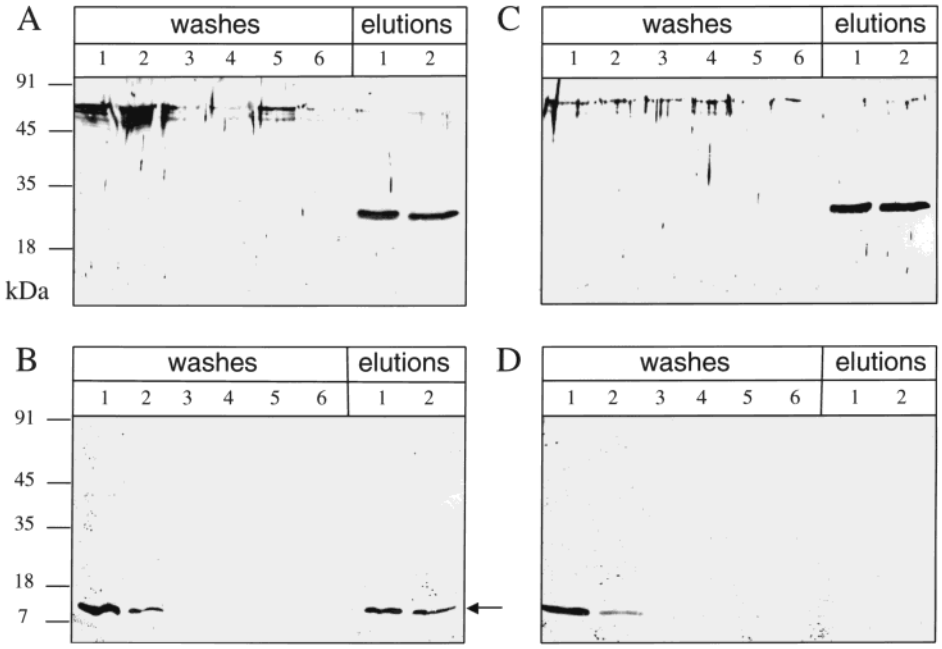

FIGURE 4: Analysis of the effects of mutations in the BRCT domain of DNA ligase III on the interaction with XRCC1. Typical results are shown for the binding, or absence of binding, between the BRCT domain of DNA ligase III (A and B), or a DNA ligase III mutant (Leu2 to His; C and D), and the XRCC1 BRCT domain. The co-affinity precipitation of the XRCC1 (arrowed) was as described in Figure 3 (B and D); the DNA ligase III in elutions was detected by specific antibodies rather than by silver staining (A and C).

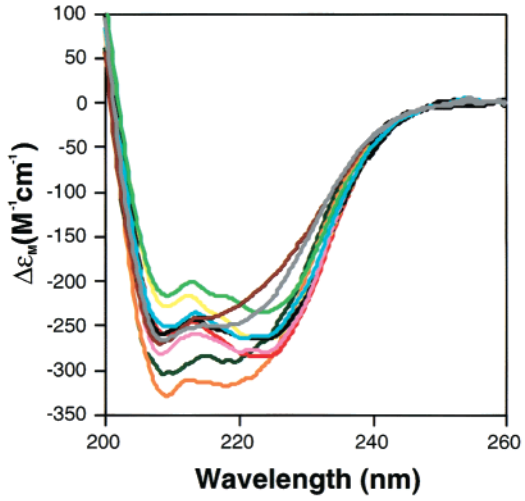

FIGURE 5: Far-UV CD spectra of mutant XRCC1 BRCT domains. Spectra were measured for XRCC1 wild-type and mutant BRCT domains as described in Experimental Procedures. The wild-type CD spectrum is shown in red. Mutants are designated as follows: Thr30Ala31 to ArgArg, orange; Leu2 to His, yellow; Arg23Arg27 to GluGlu, dark green; Trp74 to Leu, brown; Trp74 to Asp, gray; Ile48 to Glu, blue; Leu85 to His, light green; Asp20 to Ala, black; Glu59 to Lys, pink.

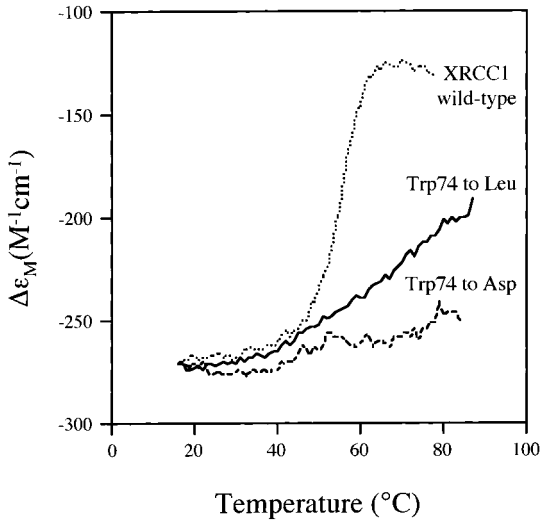

FIGURE 6: Thermal unfolding of XRCC1 BRCT domain Trp74 mutants. XRCC1 wild-type and mutant BRCT domains (as indicated) were heated to 90 °C and unfolding monitored by far-UV CD measurements at 223 nm.

interface, it was still possible that the BRCT structure had become distorted within the centrally located β-sheets, as such changes would not be detected by far-UV CD measurements. Substitution of the Trp residue did alter the thermal unfolding properties of the mutant XRCC1 BRCT domains; only the wild-type domain showed a major and reversible loss of α-helicity on heating. Furthermore, the Trp74 to Asp mutant was ~20-fold more sensitive to proteolytic digestion by trypsin compared to the wild-type XRCC1 BRCT domain (data not shown), indicating a less compact fold of the mutant BRCT domain to expose further protease-sensitive sites. Thus, it would appear that substitutions of the conserved Trp residue cause unfolding of the hydrophobic core of the BRCT domain, which indirectly affects the interaction surface and so perturbs the BRCT interface with other protein molecules.

As BRCT domains are found in proteins with diverse functions that may participate in multiple overlapping pathways, it remains a possibility that particular BRCT domains may afford other protein−protein interaction sites, in addition to the interface first identified from the XRCC1 homodimer (*16*). An alternative crystal form for the XRCC1 BRCT domain homodimer has been identified (*17*), showing an additional packing arrangement formed through the c1 and c3 surface loops (Figure 1). A mutation predicted to disrupt this secondary XRCC1 BRCT domain interface (Glu16 to Lys in loop c1) had no effect on binding to the DNA ligase III BRCT domain (data not shown). Further-

more, we have shown here that the originally identified interaction surface in the XRCC1 BRCT domain homodimer mediates the α1−α1 XRCC1−DNA ligase III heterodimer interface. The secondary interface may be involved in additional protein−protein contacts with at present unknown partners or interactions between BRCT duplicates and tandem repeats (*17*). Tandem BRCT domains have been shown to bind directly to DNA strand breaks (*31*); this is unlikely to be relevant to XRCC1−DNA ligase III, where both proteins can bind DNA through nonBRCT domains (*13*, *32*).

Many proteins containing BRCT domains interact with specific protein partners and these may occur through homo/hetero BRCT−BRCT or BRCT−nonBRCT interactions. Here we have identified a heterodimeric BRCT−BRCT interface mediating the interaction of the XRCC1−DNA ligase III DNA repair proteins. Generally, there is limited primary amino acid sequence conservation between BRCT family members, although this is more significant between XRCC1 and DNA ligase III, especially of residues contributing to the heterodimer interface (*17*). This suggests additional evolutionary constraints on the BRCT fold to preserve a functional BRCT−BRCT interaction of XRCC1−DNA ligase III that is required in BER (*4*−*6*). Nevertheless, modeling/mutagenesis based on the available XRCC1 BRCT domain structure may allow a more detailed characterization of BRCT modules mediating other protein−protein interactions. The next challenge will be to understand how such interactions are regulated (*33*, *34*) in the coordinated cellular response to DNA damage.

ACKNOWLEDGMENT

We thank Dinah Rahman for mass spectrometric confirmation of amino acid replacements.

REFERENCES

1. Koonin, E. V., Altschul, S. F., and Bork, P. (1996) *Nat. Genet. 13*, 266−268.
2. Bork, P., Hofmann, K., Bucher, P., Neuwald, A. F., Altschul, S. F., and Koonin, E. V. (1997) *FASEB J. 11*, 68−76.
3. Callebaut, I., and Mornon, J. P. (1997) *FEBS Lett. 400*, 25−30.
4. Lindahl, T., and Wood, R. D. (1999) *Science 286*, 1897−1905.
5. Caldecott, K. W., McKeown, C. K., Tucker, J. D., Ljungquist, S., and Thompson, L. H. (1994) *Mol. Cell. Biol. 14*, 68−76.
6. Nash, R. A., Caldecott, K. W., Barnes, D. E., and Lindahl, T. (1997) *Biochemistry 36*, 5207−5211.
7. Aravind, L., Walker, D. R., and Koonin, E. V. (1999) *Nucleic Acids Res. 27*, 1223−1242.
8. Thompson, L. H., Brookman, K. W., Jones, N. J., Allen, S. A., and Carrano, A. V. (1990) *Mol. Cell. Biol. 10*, 6160−6171.
9. Thompson, L. H., and West, M. G. (2000) *Mutat. Res. 459*, 1−18.
10. Wei, Y.-F., Robins, P., Carter, K., Caldecott, K. W., Pappin, J. C., Yu, G.-L., Wang, R.-P., Shell, B. K., Nash, R. A., Schar, P., Barnes, D. E., Haseltine, W. A., and Lindahl, T. (1995) *Mol. Cell. Biol. 15*, 3206−3216.
11. Mackey, Z. B., Ramos, W., Levin, D. S., Walter, C. A., McCarrey, J. R., and Tomkinson, A. E. (1997) *Mol. Cell. Biol. 17*, 989−998.
12. Masson, M., Niedergang, C., Schreiber, V., Muller, S., Menissier-de Murcia, J., and de Murcia, G. (1998) *Mol. Cell. Biol. 18*, 3563−3571.
13. Marintchev, A., Mullen, M. A., Maciejewski, M. W., Pan, B., Gryk, M. R., and Mullen, G. P. (1999) *Nat. Struct. Biol. 6*, 884−893.
14. Taylor, R. M., Moore, D. J., Whitehouse, J., Johnson, P., and Caldecott, K. W. (2000) *Mol. Cell. Biol. 20*, 735−740.
15. Tebbs, R. S., Flannery, M. L., Meneses, J. J., Hartmann, J. D., Tucker, L. H., Thompson, L. H., Cleaver, J. E., and Pedersen, R. A. (1999) *Dev. Biol. 208*, 513−529.
16. Zhang, X., Morera, S., Bates, P. A., Whitehead, P. C., Coffer, A. I., Hainbucher, K., Nash, R. A., Sternberg, M. J. E., Lindahl, T., and Freemont, P. S. (1998) *EMBO J. 17*, 6404−6411.
17. Huyton, T., Bates, P. A., Zhang, X, Sternberg, M. J. E., and Freemont, P. S. (2000) *Mutat. Res. 460*, 319−332.
18. van Ham, S. M., Tjin, E. P. M., Lillemeier, B. F., Gruneberg, U., van Meijagaarden, K. E., Pastoors, L., Verwoerd, D., Tulp, A., Canas, B., Rahman, D., Ottenhoff, T. H., Pappin, D. J., Trowsdale, J., and Neefjes, J. (1997) *Curr. Biol. 7*, 950−957.
19. Bates, P. A., and Sternberg, M. J. E. (1999) *Proteins 37* (Suppl. 3), 47−54.
20. Laskowski, R. A., MacArthur, M. W., Moss, D. S., and Thornton, J. M. (1993) *J. Appl. Crystallogr. 26*, 283−291.
21. Jones, T. A., and Kleywegt, G. J. (1999) *Proteins 37* (Suppl 3), 30−46.
22. Gill, S. C., and von Hippel, P. H. (1989) *Anal. Biochem. 182*, 319−326.
23. Caldecott, K. W., Tucker, J. D., Stanker, L. H., and Thompson, L. H. (1995) *Nucleic Acids Res. 23*, 4863−4843.
24. Taylor, R. M., Wickstead, B., Cronin, S., and Caldecott, K. W. (1998) *Curr. Biol. 8*, 877−880.
25. Moore, D. J., Taylor, R. M., Clements, P., and Caldecott, K. W. (2000) *Proc. Natl. Acad. Sci. U.S.A. 97*, 13649−13654.
26. Anderson, S. F., Schlegel, B. P., Nakajima, T., Wolpin, E. S., and Parvin, J. D. (1998) *Nat. Genet. 19*, 254−256.
27. Yu, X., Wu, L. C., Bowcocks, A. M., Aronheim, A., and Baer, R. (1998) *J. Biol. Chem. 273*, 25388−25392.
28. Hayes, F., Cayanan, C., Barilla, D., and Monteiro, A. V. N. (2000) *Cancer Res. 60*, 2411−2418.
29. Janin, J. (1997) *Nat. Struct. Biol. 4*, 973−974.
30. Woody, R. W. (1994) *Eur. Biophys. J. 23*, 253−262.
31. Yamane, K., and Tsuruo, T. (1999) *Oncogene 18*, 5194−5203.
32. Mackey, Z. B., Niedergang, C., Menissier-de Murcia, J., Leppard, J., Au, K., Chen, J., de Murcia, G., and Tomkinson, A. E. (1999) *J. Biol. Chem. 274*, 21679−21687.
33. Soulier, J., and Lowndes, N. F. (1999) *Curr. Biol. 9*, 551−554.
34. Li, S., Ting, N. S. Y., Zheng, L., Chen, P.-L., Ziv, Y., Shiloh, Y., Lee, E. Y.-H. P., and Lee, W.-H. (2000) *Nature 406*, 210−215.

BI002701E